Fabrication of Metal-Organic Framework-Containing Silica-Colloidal Crystals for Vapor Sensing

*Guang Lu, Omar K. Farha, Lauren E. Kreno, Paul M. Schoenecker, Krista S. Walton, Richard P. Van Duyne, and Joseph T. Hupp**

Metal-organic frameworks (MOFs) are a class of hybrid materials characterized by extraordinarily large surface areas, high porosity, and structural variety.[1] These properties can lead to high guest uptake, making MOFs promising materials for applications such as gas storage,[2] gas and small molecule separations,[3] heterogeneous catalysis,[4] and chemical sensing.[5,6] The excellent sorption kinetics, reversibility, and guest-induced changes in the MOF structure and/or properties make them intriguing candidates, in particular, for sensing. However, only a few of these changes (mainly luminescence quenching) have been explored for sensing purposes due to their small magnitude or the difficulty in their measurement. Integrating MOFs into devices will allow the measurement of these changes due to the uptake of guest molecules.[6] For example, the effective refractive index of a MOF should be sensitive to volatile molecules due to pore filling. This can lead to MOF-based optical devices for sensing these guest molecules. Here, we report an approach based on MOF-enshrouded colloidal crystals. Elsewhere we have described MOF-based sensors that rely upon the refractive-index modulation of Fabry–Pérot interference peaks or localized surface plasmon extinction peaks.[7]

Colloidal crystals (CCs) consist of sub-micrometer-sized silica or polymer microspheres in ordered arrays that are capable of reflecting light at a specific wavelength (stop band) due to the periodic variation of the refractive index in the crystals.[8] Colloidal crystals have been extensively studied and explored as potential sensors due to the sensitivity of the stop band to changes in their effective refractive index and/or lattice spacing. For instance, the stop band of a given colloidal crystal can be serially manipulated by loading different solvents into the pores within crystal.[9] Many functional materials, such as polymers, have been incorporated into colloidal crystals to form composites, which are capable of sensing ions,[10] biomolecules,[11] and volatile molecules[12] based on change in the refractive index of a swelled polymer and/or the lattice spacing of the crystals. In this study, we demonstrate the fabrication of MOF-silica colloidal crystal (MOF-SCC) composites and their capability of sensing volatile molecules. HKUST-1, a permanently microporous MOF with the empirical formula $Cu_2(BTC)_3$,[13] was the MOF chosen because of its well-studied structure and sorption properties,[14] large surface area, high porosity,[15] and high capacity for some harmful gases.[16] Also attractive was the availability of techniques for growing this MOF in thin-film form.[17,18] Silica was chosen as the second component of the composite due its stability and inertness with respect to volatile molecules. HKUST-1 was grown on the colloidal crystal via the step-by-step technique.

The colloidal crystal thin film was assembled from monodisperse silica microspheres via vertical deposition[19] and briefly sintered at 600 °C to enhance its mechanical stability and also to eliminate micropores in the silica microspheres.[20] Silanization and oxidation were carried out to modify the surface of microspheres with carboxylic acid groups.[21,22] The functionalized colloidal crystal film was alternately soaked in the ethanol solution of copper (II) acetate and the ethanol solution of 1,3,5-benzenetricarboxylic acid (BTC) to grow HKUST-1 on the crystal. Visible and near-infrared (IR) extinction spectra (**Figure 1**) show that the stop band of the colloidal crystal red shifts linearly with increasing the number of MOF-growth cycles. X-ray diffraction (XRD) data (**Figure 2**a) confirm the crystalline nature and identity of the MOF material grown on the colloidal crystal. The diffraction pattern for the MOF-SCC is essentially identical to that for a bulk sample of HKUST-1, apart from broadening of the peaks in the case of MOF-SCC, indicating smaller grain size. After 24 cycles of deposition of MOF material, the silica microspheres were still ordered in the typical hexagonal array, corresponding to the (111) plane of the face-centered cubic (fcc) structure, as shown in the scanning electron microscopy (SEM) image (Figure 2b). The high-magnification top-view image of the MOF-colloidal crystal film reveals that silica microspheres were coated with intergrown crystals with sizes of approximately 50 to 100 nm (Figure 2c), consistent with XRD results. Although the top surface of the composite material is rough, the MOF/microsphere interface is smooth (Figure 2d). The SEM results also reveal that the MOF material grew homogeneously throughout the colloidal crystal thin film.

At normal incidence the wavelength (λ) of the stop band in the [111] direction of a colloidal crystal is given by:

$$\lambda = \frac{2\sqrt{2}}{\sqrt{3}} n D \quad (1)$$

where n is the effective refractive index of the colloidal crystal and D is the diameter of microsphere. One of the keys to chemical sensing is the tunability of n. For the MOF-SCCs, n is a

Dr. G. Lu, Prof. O. K. Farha, L. E. Kreno, Prof. R. P. Van Duyne, Prof. J. T. Hupp
Department of Chemistry
Northwestern University
2145 Sheridan Road, Evanston, IL 60208, USA
E-mail: j-hupp@northwestern.edu
P. M. Schoenecker, Prof. K. S. Walton
School of Chemical and Biomolecular Engineering
Georgia Institute of Technology
Atlanta, GA 30332, USA

DOI: 10.1002/adma.201102116

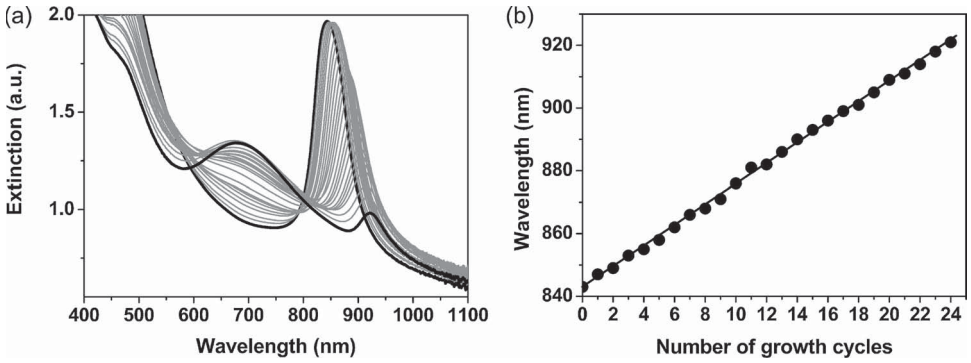

Figure 1. a) Visible and near-IR extinction spectra of the MOF-silica colloidal crystal thin film prepared via the step-by-step technique. b) The stop band of the colloidal crystal versus the number of MOF-growth cycles.

volume-weight average of indices for the silica microspheres ($n_{SiO_2} > 1$), metal-organic framework ($n_{fram} > 1$), and cavities (including micropores in framework and mesopores between MOF-coated silica spheres) (vacuum, $n_{vac} = 1$) and is given by:

$$n = \sqrt{f_{SiO_2} n_{SiO_2}^2 + f_{fram} n_{fram}^2 + (1 - f_{SiO_2} - f_{fram}) n_{vac}^2} \quad (2)$$

where f_{SiO_2} and f_{fram} are the volume fractions of the silica microspheres and the metal-organic framework, respectively. Sorption of volatile molecules (refractive index $n_a > 1$) by MOF will displace vacuum within the microporous framework and increase effective refractive index. This will result in red shifts of the stop band according to Equation 1.

Since HKUST-1 can adsorb significant amounts of water from the ambient atmosphere, the MOF-SCCs were subjected to a high-rate flow of dry nitrogen prior to exposure to analyte vapors. Consistent with removal of water and/or residual solvent, the MOF-SCC stop band exhibited a blue shift of a few nanometers in response to nitrogen drying.

Figure 3a shows that the stop band of the MOF-SCC red shifts by up to ≈16 nm upon exposure to carbon disulfide (CS_2), with the largest shifts occurring at the highest vapor concentrations. This observation is consistent with an increase in the effective refractive index of the microporous MOF due to uptake of CS_2. Importantly, control experiments with an unmodified silica colloidal crystal show essentially no change in its stop band

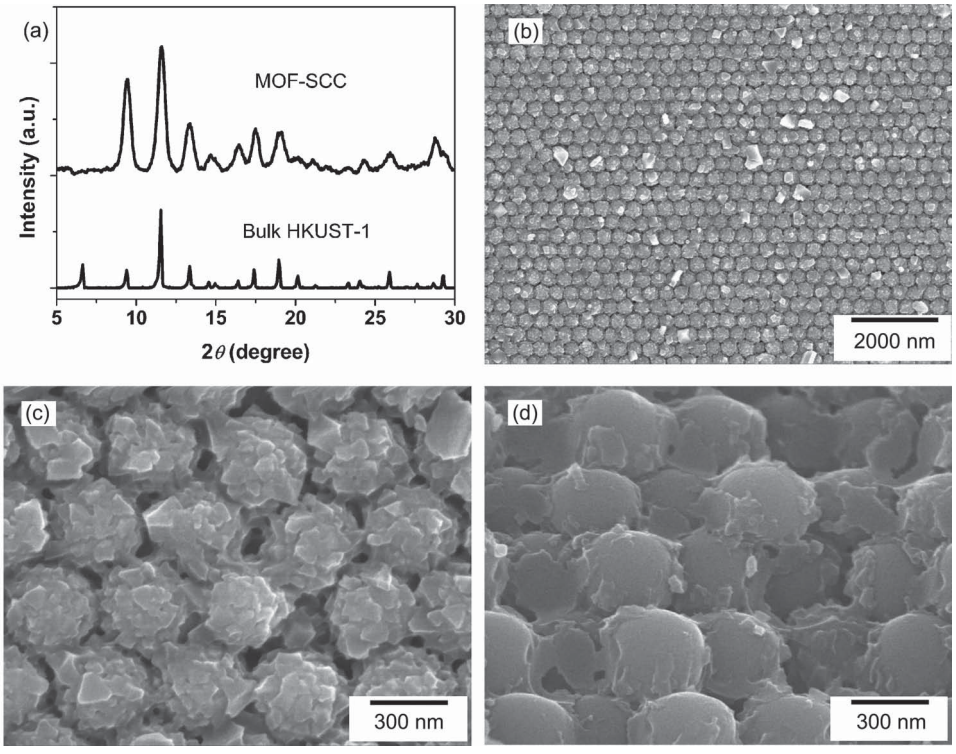

Figure 2. a) X-ray diffraction (XRD) patterns of MOF-silica colloidal crystal thin film (top) and HKUST-1 bulk crystal prepared via conventional solvothermal procedure (bottom). SEM images of the MOF-silica colloidal crystal thin film: b) top view at low magnification, c) top view at high magnification, and d) cross-sectional view at high magnification.

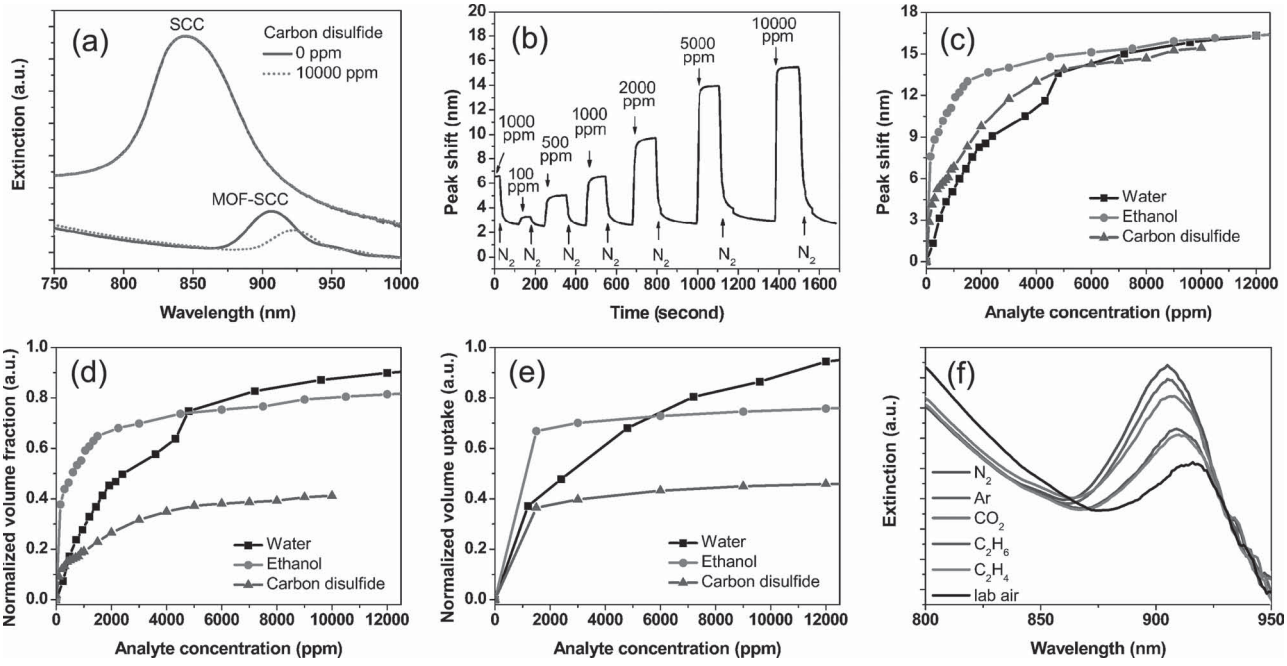

Figure 3. a) Near-IR extinction spectra of the MOF-silica colloidal crystal thin film and the unmodified colloidal crystal thin film before and after exposure to 10 000 ppm carbon disulfide. b) Responses of MOF-silica colloidal crystal thin film to a series of CS_2 vapors of various concentrations versus time. c) Dependence of the stop-band shift of the MOF-silica colloidal crystal thin film on the concentrations of vapors of water, ethanol, and carbon disulfide and d) corresponding normalized vapor adsorption curves. e) Normalized vapor adsorption curves for water, ethanol, and carbon disulfide by HKUST-1 thin film grown on a quartz crystal microbalance electrode. f) Near-IR extinction spectra of MOF-silica colloidal crystal thin film on exposure to various gases showing a stop band at 904 nm for nitrogen, 905 nm for argon, 907 nm for carbon dioxide, 909 nm for ethane, 910 nm for ethylene, and 917 nm for laboratory air, respectively.

upon exposure to CS_2. As shown in Figure 3b, the MOF-SCC response is rapid (seconds) and reversible to analyte vapors. Measurable single-wavelength signals were easily obtained from 100 ppm CS_2 (the lowest concentration examined). We have estimated potential detection limits based on stop-band peak shifts with our high-resolution spectrometer (with a shift resolution $3\sigma = 0.015$ nm). These are: 2.6 ppm (water), 0.5 ppm (carbon disulfide), and 0.3 ppm (ethanol).

Figure 3c shows the responses of a thin-film MOF-SCC sample to a series of vapors of various concentrations for CS_2, ethanol, and water. The magnitudes of the red shifts of the stop band for the three tested analytes are different at vapor concentrations lower than 10 000 ppm, but become similar at higher concentration. In order to reveal the nature of the analyte-induced shifts of the stop band of MOF-SCCs, we calculated and normalized the volume fractions of analytes adsorbed in the MOF from Equation 1 and Equation 2 to construct the adsorption curves shown in Figure 3d. Notably, their shapes agree well with the shapes of the adsorption curves measured by quartz crystal microgravimetry (QCM) for thin films of HKUST-1 (Figure 3e and Figure S2 in the Supporting Information, which also contains data (Figure S3) showing very good agreement between curves measured by stop-band shifts versus dedicated vapor sorption instrumentation). For reasons that are unclear, MOF-SCC and QCM films of HKUST-1 both exhibited significantly less adsorption of CS_2 than of water or ethanol. Nevertheless, the maximum shifts of the stop band are similar for the three compounds, reflecting the fact that the shifts depend on both the amount of analytes adsorbed and their refractive index (1.63 for carbon disulfide, 1.36 for ethanol, and 1.33 for water).

In addition to vapors, the stop bands of MOF-SCCs should be sensitive to gases that are sorbed. As shown in Figure 3f, following flushing with dry nitrogen, which is insignificantly sorbed at ambient temperature, measurable stop-band red shifts were indeed observed when the sample was exposed to any of several gases including laboratory air, argon, carbon dioxide, ethane, and ethylene.

In summary, permanently microporous MOFs are potentially useful materials for monitoring or sensing gases and volatile chemical compounds. By combining MOFs with thin-film colloidal crystals, the challenge of signal transduction in response to molecular sorption by the MOF can be met. We have demonstrated the concept here by using HKUST-1 in combination with silica nanospheres configured as thin-film colloidal crystals. Shifts in the colloidal crystal stop band are readily observed upon analyte (vapor or gas) sorption by the microporous MOF. The responses are reversible and have been validated by quartz crystal microgravimetry measurements. Following this proof-of-concept, it should be possible to use appropriately pore-tailored MOFs to engender chemically specific sensor responses.

Experimental Section

Silica microspheres were synthesized using a modified Stöber method[23] and the colloidal crystal thin films were grown on glass slides using

vertical deposition technique.[19] The resulting colloidal crystal thin films were briefly sintered at high temperature and subsequently functionalized with carboxylic acid groups by hydroxylation, silanization, and oxidation (see Supporting Information).

The carboxylic acid functionalized colloidal crystal film was immersed in a solution of copper (II) acetate (1 mM) in ethanol for 30 min and then in a solution of 1,3,5-benzenetricarboxylic acid (1 mM) in ethanol for 60 min. Between each immersion, the film was rinsed thoroughly with ethanol and dried under flowing nitrogen. This process was repeated and a typical film underwent 24 cycles of growth.

The MOF-colloidal crystal film was placed in a home-built small-volume (≈1.1 mL) aluminum measurement cell with a TorrSeal adhered quartz window, which was mounted in either a Cary 50 Bio UV-visible spectrophotometer or a home-built high-resolution spectrophotometer.[24] Prior to introducing analyte vapors, the cell atmosphere was exchanged with nitrogen at high flow rate (≈20 SCFH) for 10 min to remove remaining solvent molecule and/or moisture in the composite. Source vapor samples (24 000 ppm for water, 15 000 ppm for ethanol, and 10 000 ppm for CS_2) were prepared by injection of a measured volume of liquids (0.77 mL for water, 1.56 mL for ethanol, and 1.08 mL for CS_2) into a ≈40 L vapor dilution bag (2-mil Tedlar, Pollution Measurement Corporation, Oak Park, IL), followed by inflation with dry nitrogen to a known volume (40 L). A series of vapors of known concentrations were obtained by diluting the above-described source samples with dry nitrogen using a Model 1010 Precision Gas Diluter (Custom Sensor Solutions, Inc., Naperville, IL) and then delivered (at flow rate of ≈200 sccm) to the measurement cell containing the MOF-colloidal crystal composite film by using a Model 1011 Gas Sample Pump (Custom Sensor Solutions, Inc., Naperville, IL) and Bev-A-Line IV chemical-resistant tubing (Cole-Parmer, Vernon Hills, IL). The stop band of the MOF-colloidal crystal was monitored via the high-resolution spectrophotometer or the commercial spectrophotometer at room temperature. Gas sensing was done in a similar fashion to vapor sensing, except utilizing mass flow controllers in order to fix the flow rate (total 100 sccm) of gas.

HKUST-1 thin films were also grown on gold electrodes used for QCM, in order to provide an alternative means of measuring vapor adsorption.[25] The MOF-coated QCM electrode was mounted on a polypropylene QCM holder (FC-550 Flow Cell, Maxtekinc Inc., CA) and purged with nitrogen at a flow rate of about 20 SCFH for 10 min prior to introducing vapor samples. Vapor samples with known concentrations were prepared as outlined above. Changes in frequency and mass of the MOF-coated QCM electrode on exposing to vapor were recorded on a Research Quartz Crystal Microbalance (Maxtekinc. Inc., CA).

Supporting Information

Supporting Information is available from the Wiley Online Library or from the author.

Acknowledgements

The authors thank DTRA (grant HDTRA1-09-01-0007), AFOSR, and the Northwestern Nanoscale Science and Engineering Center for support of our work. L.E.K. thanks the Dept. of Defense for an NDSEG Fellowship.

Received: June 6, 2011
Published online:

[1] a) J. L. C. Rowsell, O. M. Yaghi, *Microporous Mesoporous Mater.* **2004**, *73*, 3; b) G. Feréy, *Chem. Soc. Rev.* **2008**, *37*, 191; c) O. K. Farha, J. T. Hupp, *Acc. Chem. Res.* **2010**, *43*, 1166; d) S. Kitagawa, R. Kitaura, S. Noro, *Angew. Chem. Int. Ed.* **2004**, *43*, 2334.
[2] a) L. J. Murray, M. Dinča, J. R. Long, *Chem. Soc. Rev.* **2009**, *38*, 1294; b) D. J. Collins, H.-C. Zhou, *J. Mater. Chem.* **2007**, *17*, 3154.
[3] J.-R. Li, R. J. Kuppler, H.-C. Zhou, *Chem. Soc. Rev.* **2009**, *38*, 1477.
[4] a) J. Y. Lee, O. K. Farha, J. Roberts, K. A. Scheidt, S. T. Nguyen, J. T. Hupp, *Chem. Soc. Rev.* **2009**, *38*, 1450; b) L. Ma, C. Abney, W. Lin, *Chem. Soc. Rev.* **2009**, *38*, 1248.
[5] a) B. L. Chen, Y. Yang, F. Zapata, G. N. Lin, G. D. Qian, E. B. Lobkovsky, *Adv. Mater.* **2007**, *19*, 1693; b) B. L. Chen, L. B. Wang, F. Zapata, G. D. Qian, E. B. Lobkovsky, *J. Am. Chem. Soc.* **2008**, *130*, 6718; c) B. L. Chen, L. B. Wang, Y. Q. Xiao, F. R. Fronczek, M. Xue, Y. J. Cui, G. D. Qian, *Angew. Chem. Int. Ed.* **2009**, *48*, 500; d) B. V. Harbuzaru, A. Corma, F. Rey, J. L. Jordá, D. Ananias, L. D. Carlos, J. Rocha, *Angew. Chem. Int. Ed.* **2009**, *48*, 6476; e) B. V. Harbuzaru, A. Corma, F. Rey, P. Atienzar, J. L. Jordá, H. García, D. Ananias, L. D. Carlos, J. Rocha, *Angew. Chem. Int. Ed.* **2008**, *47*, 1080; f) W. J. Rieter, K. M. L. Taylor, W. B. Lin, *J. Am. Chem. Soc.* **2007**, *129*, 9852; g) Z. Xie, L. Ma, K. E. deKrafft, A. Jin, W. Lin, *J. Am. Chem. Soc.* **2010**, *132*, 922; h) K. L. Wong, G. L. Law, Y. Y. Yang, W. T. Wong, *Adv. Mater.* **2006**, *18*, 1051; i) B. Zhao, X. Y. Chen, P. Cheng, D. Z. Liao, S. P. Yan, Z. H. Jiang, *J. Am. Chem. Soc.* **2004**, *126*, 15394.
[6] M. D. Allendorf, R. J. T. Houk, L. Andruszkiewicz, A. A. Talin, J. Pikarsky, A. Choudhury, K. A. Gall, P. J. Hesketh, *J. Am. Chem. Soc.* **2008**, *130*, 14404.
[7] a) G. Lu, J. T. Hupp, *J. Am. Chem. Soc.* **2010**, *132*, 7832; b) L. E. Kreno, J. T. Hupp, R. P. Van Duyne, *Anal. Chem.* **2010**, *82*, 8042.
[8] Y. Xia, *Adv. Mater.* **2001**, *13*, 369.
[9] J. Li, W. Huang, Z. Wang, Y. Han, *Colloids Surf. A: Physicochem. Eng. Aspects* **2007**, *293*, 130.
[10] a) J. H. Holtz, S. A. Asher, *Nature* **1997**, *389*, 829; b) S. A. Asher, A. C. Sharma, A. V. Goponenko, M. M. Ward, *Anal. Chem.* **2003**, *75*, 1676.
[11] A. C. Sharma, T. Jana, R. Kesavamoorthy, L. Shi, M. A. Virji, D. N. Finegold, S. A. Asher, *J. Am. Chem. Soc.* **2004**, *126*, 2971.
[12] a) E. Tian, J. Wang, Y. Zheng, Y. Song, L. Jiang, D. Zhu, *J. Mater. Chem.* **2008**, *18*, 1116; b) A. C. Arsenault, V. Kitaev, I. Manners, G. A. Ozin, A. Mihi, H. Míguez, *J. Mater. Chem.* **2005**, *15*, 133.
[13] S. S.-Y. Chui, S. M.-F. Lo, J. P. H. Charmant, A. G. Orpen, I. D. Williams, *Science* **1999**, *283*, 1148.
[14] a) Q. M. Wang, D. Shen, M. Bülow, M. L. Lau, S. Deng, F. R. Fitch, N. O. Lemcoff, J. Semanscin, *Microporous Mesoporous Mater.* **2002**, *55*, 217; b) J. R. Karra, K. S. Walton, *Langmuir* **2008**, *24*, 8620.
[15] a) J. C. Liu, J. T. Culp, S. Natesakhawat, B. C. Bockrath, B. Zande, S. G. Sankar, G. Garberoglio, J. K. Johnson, *J. Phys. Chem. C* **2007**, *111*, 9305; b) T. Düren, F. Millange, G. Férey, K. S. Walton, R. Q. Snurr, *J. Phys. Chem. C* **2007**, *111*, 15350.
[16] a) D. Britt, D. Tranchemontagne, O. M. Yaghi, *Proc. Natl. Acad. Sci. USA* **2008**, *105*, 11623; b) B. Xiao, P. S. Wheatley, X. Zhao, A. J. Fletcher, S. Fox, A. G. Rossi, I. L. Megson, S. Bordiga, L. Regli, K. M. Thomas, R. E. Morris, *J. Am. Chem. Soc.* **2007**, *129*, 1203.
[17] O. Shekhah, H. Wang, S. Kowarik, F. Schreiber, M. Paulus, M. Tolan, C. Sternemann, F. Evers, D. Zacher, R. A. Fischer, C. Wöll, *J. Am. Chem. Soc.* **2007**, *129*, 15118.
[18] E. Biemmi, C. Scherb, T. Bein, *J. Am. Chem. Soc.* **2007**, *129*, 8054.
[19] P. Jiang, J. F. Bertone, K. S. Hwang, V. L. Colvin, *Chem. Mater.* **1999**, *11*, 2132.
[20] A. A. Chabanov, Y. Jun, D. J. Norris, *Appl. Phys. Lett.* **2004**, *84*, 3573.
[21] J. F. Mooney, A. J. Hunt, J. R. Mcintosh, C. A. Liberko, D. M. Walba, C. T. Rogers, *Proc. Natl. Acad. Sci. USA* **1996**, *93*, 12287.
[22] S. R. Wasserman, Y. -T. Tao, G. M. Whitesides, *Langmuir* **1989**, *5*, 1074.
[23] a) W. Stöber, A. Fink, E. Bohn, *J. Colloid Interface Sci.* **1968**, *26*, 62; b) H. Giesche, *J. Eur. Ceram. Soc.* **1994**, *14*, 205.
[24] J. N. Anker, W. P. Hall, M. P. Lambert, P. T. Velasco, M. Mrksich, W. L. Klein, R. P. Van Duyne, *J. Phys, Chem. C* **2009**, *113*, 5891.
[25] E. Biemmi, A. Darga, N. Stock, T. Bein, *Microporous Mesoporous Mater.* **2008**, *114*, 380.